

Available online at [www.sciencedirect.com](http://www.sciencedirect.com)**ScienceDirect**

Journal of the Chinese Medical Association 78 (2015) 726–731

[www.jcma-online.com](http://www.jcma-online.com)

Original Article

# Efficacy of gadoxetic acid-enhanced magnetic resonance cholangiography compared with T2-weighted magnetic resonance cholangiography in patients with liver cirrhosis

Wen-Pei Wu <sup>a,b</sup>, Ran-Chou Chen <sup>b,c</sup>, Chih-Wei Lee <sup>d</sup>, Yao-Li Chen <sup>e</sup>, Kwo-Whei Lee <sup>d</sup>,  
Hwa-Koon Wu <sup>d</sup>, Chen-Te Chou <sup>b,d,\*</sup>

<sup>a</sup> Department of Radiology, Lukang Christian Hospital, Chang-Hua, Taiwan, ROC

<sup>b</sup> Department of Biomedical Imaging and Radiological Sciences, National Yang-Ming University, Taipei, Taiwan, ROC

<sup>c</sup> Department of Radiology, Heping Fuyou Branch, Taipei City Hospital, Taipei, Taiwan, ROC

<sup>d</sup> Department of Radiology, Chang-Hua Christian Hospital, Chang-Hua, Taiwan, ROC

<sup>e</sup> Transplant Center, Chang-Hua Christian Hospital, Chang-Hua, Taiwan, ROC

Received March 9, 2014; accepted June 16, 2015

## Abstract

**Background:** Gadoxetic acid is one of the hepatobiliary-specific agents and so can be used for contrast-enhanced magnetic resonance cholangiography (CE-MRC). The aim of our study was to compare the performance of CE-MRC with that of T2-weighted magnetic resonance cholangiography (T2W-MRC), and also to ascertain the effectiveness of both modalities combined for visualizing anatomic structures of the biliary tree in patients with liver cirrhosis.

**Methods:** Fifty-six patients underwent CE-MRC and T2W-MRC imaging. In the CE-MRC studies, hepatobiliary phase images were acquired 20 minutes after contrast injection. Two radiologists first evaluated the T2W-MRC and CE-MRC images separately in random order, and then they reviewed both images together 8 weeks later. The readers graded the quality of visualization of each biliary duct and the entire biliary tree (overall rating) using a five-point scale. Images with a grade of 3 or 4 were considered to provide sufficient visualization for clinical application, and those with a grade of 2 or less were considered to provide insufficient visualization. Laboratory data, Child–Pugh classification, and model for end-stage liver disease score were also recorded.

**Results:** The overall rating of T2W-MRC was significantly higher than that of CE-MRC ( $p < 0.001$ ), although combined T2W/CE-MRC provided better visualization of biliary segments than T2W-MRC alone ( $p = 0.025$ ). There were no significant differences between liver function and the overall rating of CE-MRC.

**Conclusion:** CE-MRC is not superior to conventional T2W-MRC with respect to biliary visualization in patients with liver cirrhosis. However, a combination of T2W-MRC and CE-MRC provides significantly better visualization of biliary structures than T2W-MRC alone.

Copyright © 2015 Elsevier Taiwan LLC and the Chinese Medical Association. All rights reserved.

**Keywords:** gadoxetic acid; liver cirrhosis; magnetic resonance cholangiography

## 1. Introduction

T2-weighted magnetic resonance cholangiography (T2W-MRC) is a widely accepted noninvasive method for imaging choledocholithiasis, biliary tract obstruction and dilatation, and biliary anatomy.<sup>1–5</sup> However, the technique is associated with several interpretive pitfalls, which may result in

Conflicts of interest: The authors declare that there are no conflicts of interest related to the subject matter or materials discussed in this article.

\* Corresponding author. Dr. Chen-Te Chou, Department of Radiology, Chang-Hua Christian Hospital, 135, Nanxiao Street, Changhua 500, Taiwan, ROC.

E-mail address: [chouchente@yahoo.com.tw](mailto:chouchente@yahoo.com.tw) (C.-T. Chou).

<http://dx.doi.org/10.1016/j.jcma.2015.06.019>

1726-4901/Copyright © 2015 Elsevier Taiwan LLC and the Chinese Medical Association. All rights reserved.

diagnostic errors.<sup>6–8</sup> In addition, T2W-MRC yields static images in contrast to real-time images obtained using endoscopic retrograde cholangiopancreatography or percutaneous transhepatic cholangiography. Moreover, T2W-MRC cannot discriminate between different kinds of fluids (for example, bile leakage from small ascites), and soft tissue contrast can be lost with a very long echo time.

Several studies have shown that contrast-enhanced magnetic resonance cholangiography (CE-MRC) has the potential to provide a “one stop shop” for diagnosing anatomic and functional abnormalities of the biliary tree.<sup>9–13</sup> Gadolinium-ethoxybenzyl-diethylenetriaminepentaacetic acid (gadoteric acid) and gadobenate dimeglumine can be used as intravascular–interstitial contrast agents for dynamic magnetic resonance imaging (MRI) and as hepatocyte-specific contrast agents for MRC. However, because of earlier onset and longer duration, gadoteric acid may provide better visualization of biliary structures within a shorter period of time than gadobenate dimeglumine.<sup>14</sup>

Recent studies have shown that CE-MRC with gadoteric acid is an effective technique for evaluating biliary tract anatomy, obstruction, and active bile leakage in patients with normal liver function.<sup>15–18</sup> Few studies, however, have investigated the quality of bile duct visualization using CE-MRC in patients with liver cirrhosis,<sup>19</sup> and to the best of our knowledge, no studies have compared the quality of visualization obtained by CE-MRC with that obtained by T2W-MRC in patients with cirrhosis. The purpose of our study was to compare the performance of CE-MRC with that of T2W-MRC, and assess the effectiveness of both modalities combined for visualizing anatomic structures of the biliary tree in patients with liver cirrhosis.

## 2. Methods

### 2.1. Patients

This retrospective study was approved by the Institutional Review Board of our hospital. A total of 60 consecutive patients underwent gadoteric acid-enhanced MRI of liver for suspected focal liver lesions during a 16-month period (from October 2008 to January 2011). The focal lesions were diagnosed either histologically or radiologically, and comprised hepatocellular carcinoma in 51 patients, hepatocholangiocarcinoma in two patients, dysplastic nodules in two patients, hemangioma in one patient, and focal nodular hyperplasia in one patient. No abnormal pathology was detected in three patients. The inclusion criteria for our study were as follows: (1) patients must have liver cirrhosis; (2) laboratory and MRI studies should have been conducted within a 2-week period; and (3) both gadoteric acid-enhanced MRC and T2W-MRC images should be available for review. A total of 56 patients fulfilled the criteria and were enrolled into the study. The cohort comprised 43 men and 13 women in the age range of 30–82 years (mean age, 59.9 years). The diagnosis of cirrhosis was established histologically in 43 patients (biopsy,  $n = 14$ ; surgical resection,  $n = 21$ ; liver

transplantation,  $n = 8$ ) and was based on the combination of clinical, laboratory, endoscopic, and ultrasound findings in 13 patients. The clinical diagnosis of liver cirrhosis was made in patients with chronic liver disease who had one or more of the following clinical findings: firm liver and ascites, signs of collateral circulation, prothrombin index  $<85\%$ , ultrasonographic evidence of irregular liver surface and heterogeneity, and endoscopic evidence of esophageal varices.<sup>20</sup> No biliary duct dilatations were observed in any of the 56 patients.

The underlying causes of liver cirrhosis were hepatitis B ( $n = 28$ ), hepatitis C ( $n = 16$ ), hepatitis B and hepatitis C combined ( $n = 4$ ), alcoholic chronic hepatitis ( $n = 4$ ), and cryptogenic cirrhosis ( $n = 4$ ). Hepatic function was classified as Child–Pugh Class A in 31 patients, Child–Pugh Class B in 13 patients, and Child–Pugh Class C in 12 patients.

### 2.2. MRI technique

All MR studies were performed with a 1.5-T MR scanner (Gyrosan ACS-NT Intera; Philips, Best, The Netherlands) and a phased-array body coil. Navigator-triggered three-dimensional (3D) T2W-MRC images were obtained during free breathing (1800/650; refocusing flip angle,  $90^\circ$ ; field of view (FOV), 300 mm; matrix,  $512 \times 512$ ; echo train length, 115; slab thickness, 80 mm; section thickness, 1 mm; interpolation to 80 sections of 1-mm intervals; parallel acquisition technique factor, 2; no phase wrap option; acquisition time, 260–300 seconds). A whole-volume maximum-intensity projection reformation was applied in the coronal plain.

For contrast-enhanced MRI with gadoteric acid, all patients received a 0.025 mmol/kg (0.1 mL/kg) dose of gadoteric acid (Primovist; Bayer Schering Pharma, Berlin, Germany). The contrast agent was administered as a manual bolus injection at a speed of approximately 2 mL/second through peripheral veins. The line was flushed with 20 mL of 0.9% saline. Dynamic 3D T1W fast-field echo imaging (repetition time (TR)/echo time (TE), 10.2–10.7 milliseconds/5 milliseconds; slice thickness, 3 mm; matrix,  $192 \times 256$ ; number of excitations (NEX), 1; flip angle,  $15^\circ$ ; FOV, 38–40 cm) was carried out before and 25–30 seconds (arterial phase), 55–60 seconds (portal phase), and 85–90 seconds (venous phase) after the injection of the contrast agent. Delayed MRI at 20 minutes after the application of gadoteric acid was performed with the same parameters as used for the dynamic study. CE-MRC images were reconstructed using a coronal oblique multiplanar reformatted image generated from the 20-minute delayed 3D T1W images.

### 2.3. Imaging evaluation

Imaging analysis was performed on a dual-screen diagnostic workstation (GE Healthcare, Milwaukee, WI, USA). Images were evaluated by two experienced radiologists (with 15 and 7 years of clinical experience in abdominal MR) who were not aware of the patients' clinical characteristics or laboratory results. Readers categorized the MRC images into three groups: T2W-MRC, CE-MRC, and a combined group (T2W-MRC plus CE-MRC). Image review was based on

source images, multiplanar reformats, and maximum intensity projections. To reduce reviewer bias, T2W-MRC and CE-MRC images were arranged in random order and evaluated separately. Approximately 8 weeks later, the radiologists reviewed the combined T2W-MRC and CE-MRC images.

The two readers were asked to evaluate all MR image sets and record the bile duct visualization grading scores. The following structures were evaluated: the common bile duct (CBD), the common hepatic duct (CHD), and the right and left hepatic ducts and their secondary branches. The quality of visualization of the bile ducts was assessed using a five-point Likert-type scale as follows: Grade 0, nonvisualization of the ducts; Grade 1, partial visualization of less than half of the duct, high to moderate artifacts, or extensive superimposition of other anatomic structures; Grade 2, visualization of more than half of the duct, few to moderate artifacts, or moderate superimposition of other anatomic structures; Grade 3, total visualization of its entire length with ambiguous margins, few artifacts, or minimal superimposition of other anatomic structures; and Grade 4, excellent visualization with clear margins.<sup>9</sup> Disagreements in imaging evaluation between the two radiologists were resolved by consensus with a third radiologist. The images of the bile ducts ranked as 3 or 4 were grouped as “sufficient visualization” for clinical application, and those ranked as 2 or less were grouped as “insufficient visualization” (Fig. 1).

In addition to grading the quality of visualization of each biliary duct, the readers also graded the visualization of the entire biliary tree (overall rating). When all the segments, including CBD, CHD, and right and left hepatic ducts, could be visualized, the overall rating was deemed to be “sufficient.” If any one of the segments could not be visualized, the overall rating was deemed insufficient.<sup>19</sup>

Patients' charts were reviewed and the following serum parameters were recorded: serum total bilirubin, platelet count, creatinine, prothrombin time, glutamic oxaloacetic transaminase, glutamic pyruvic transaminase, and albumin. Child–Pugh classification, Child–Pugh score, and model for end-stage liver disease (MELD) score were also determined for each patient. A patient's MELD score is calculated using

values for serum creatinine, total bilirubin, and the international normalized ratio as follows:  $MELD = 9.57 \times \text{Log}_e(\text{creatinine}) + 3.78 \times \text{Log}_e(\text{total bilirubin}) + 11.2 \times \text{Log}_e(\text{international normalized ratio}) + 6.43$ .<sup>21</sup>

#### 2.4. Statistical analysis

We used a weighted kappa statistic to measure interviewer agreement according to each biliary segment. Serial weighted pairwise comparisons across two reviewers were performed, and an average kappa value was calculated. A kappa value of 0.00 indicated no agreement; 0.01–0.20, slight agreement; 0.21–0.40, fair agreement; 0.41–0.60, moderate agreement; 0.61–0.80, good agreement; and 0.81–1.00, excellent agreement. Using T2W-MRC as a standard reference, the overall ratings and ratings for visualization of biliary segments were compared between CE-MRC and T2W-MRC and between the combined group and T2W-MRC using the Wilcoxon signed-rank test. Analysis of the relationships between the overall rating of CE-MRC and various liver function parameters was also performed using the Wilcoxon signed-rank test. A *p* value of <0.05 was considered to indicate statistical significance. All statistical analyses were performed using the statistical package SPSS for Windows (version 20.0.0; SPSS, Chicago, IL, USA).

### 3. Results

A total of 328 biliary segments in 56 patients were evaluated. Eight segments were missing in four patients because they had undergone right (*n* = 3) or left (*n* = 1) hemihepatectomy. The bile ducts were not visible on T2W-MRC images in three patients (5.4%) or on CE-MRC images in two patients (3.6%). The inter-reviewer agreement for the degree of segmental visualization reached good to excellent levels ( $\kappa = 0.76$ –0.94) (Table 1). In two of the three patients for whom the bile ducts were not visible on T2W-MRC images, there was sufficient visualization for anatomical diagnosis on CE-MRC images (Fig. 2).

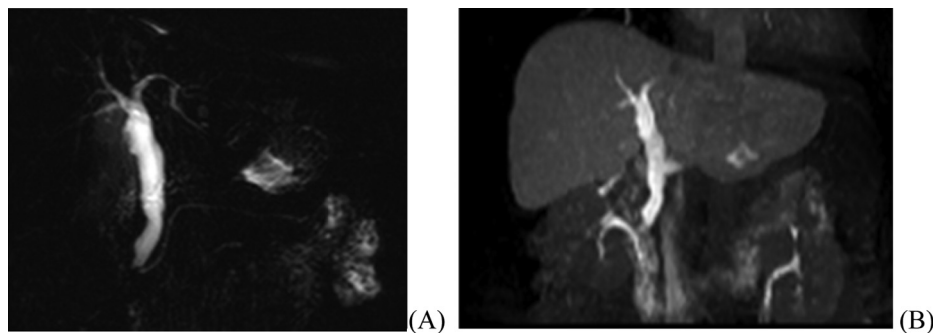


Fig. 1. A 52-year-old man with histologically proven liver cirrhosis (Child–Pugh Classification A, MELD score 7, total bilirubin, 1.17 mg/dL). (A) T2-weighted MRC clearly depicts the common bile duct, common hepatic duct, and bilateral hepatic ducts (all ranked Grade 4). (B) CE-MRC in the coronal plane demonstrates biliary excretion after application of gadoxetic acid in the hepatobiliary phase. The quality of visualization of the common bile duct, common hepatic duct, and bilateral hepatic ducts by CE-MRC was rated to be as good as the quality of visualization of those structures by T2-weighted MRC. CE-MRC = gadoxetic acid-enhanced magnetic resonance cholangiography; MELD = model for end-stage liver disease; MRC = magnetic resonance cholangiography.

Table 1  
Interobserver agreement by kappa analysis.

Segment	κ value		
	T2W-MRC	CE-MRC	Combined T2W-MRC and CE-MRC
CBD	0.94	1.00	0.93
CHD	0.90	0.76	0.78
RHD	0.87	0.85	0.82
LHD	0.92	0.74	0.76
Second branch of RHD	0.88	0.84	0.82
Second branch of LHD	0.84	0.89	0.84

CBD = common bile duct; CE-MRC = contrast-enhanced magnetic resonance cholangiography; CHD = common hepatic duct; LHD = left hepatic duct; RHD = right hepatic duct; T2W-MRC = T2-weighted magnetic resonance cholangiography.

The ratings for visualization of each biliary segment and the overall ratings in the T2W-MRC group, CE-MRC group, and combined group are shown in Table 2. For segment-based visualization of each bile duct, the combined group showed significantly better visualization of the CBD, CHD, and bilateral hepatic ducts than T2W-MRC alone. However, no

significant differences in visualization of the secondary branches were found. In addition, there were no significant differences between CE-MRC and T2W-MRC in visualization of any of the biliary segments, with the exception of the left hepatic duct ( $p = 0.004$ ).

Based on the overall rating, CE-MRC alone provided sufficient visualization of the biliary tree in only 35.7% (20/56) of patients, whereas T2W-MRC alone provided sufficient visualization in 66.1% (37/56) of patients. However, T2W-MRC/CE-MRC allowed for sufficient visualization in 71.4% (40/56) of patients. The overall rating of combined imaging was significantly better than that of T2W-MRC imaging alone ( $p = 0.025$ ), and the overall rating of T2W-MRC alone was significantly better than that of CE-MRC alone ( $p < 0.001$ ).

We then analyzed whether liver function affected the quality of visualization of the biliary tract on CE-MRC images. We found that although the number of images with insufficient visualization tended to be higher in patients with Child–Pugh classification C, higher Child–Pugh scores, higher MELD scores, and higher total bilirubin levels, there were no significant differences between liver function parameters and visualization quality (Table 3).

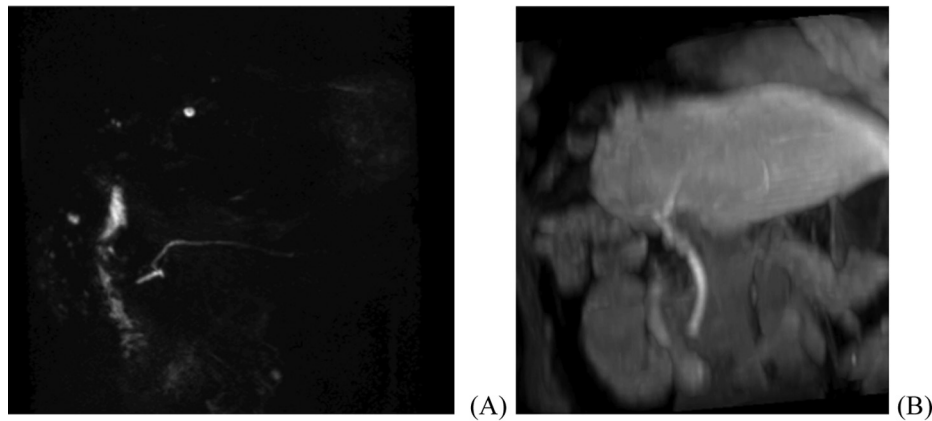


Fig. 2. An 81-year-old man with liver cirrhosis underwent right hepatic lobectomy for hepatocellular carcinoma (Child–Pugh Classification A, MELD score 12, total bilirubin, 0.75 mg/dL). (A) T2W-MRC shows no visualization of any bile ducts but clearly depicts the pancreatic duct. Lack of visualization is probably due to thick bile in the biliary tree. (B) Gadoteric acid-enhanced MRC in the coronal plane demonstrates biliary enhancement of the common bile duct, common hepatic duct, and left hepatic duct (all ranked Grade 3). Both CE-MRC alone and combined CE/T2W-MRC provided sufficient visualization. CE-MRC = gadoteric acid-enhanced magnetic resonance cholangiography; MELD = model for end-stage liver disease; MRC = magnetic resonance cholangiography; T2W-MRC = T2-weighted magnetic resonance cholangiography.

Table 2  
Diagnostic performance of the overall rating and each segment for T2W-MRC, CE-MRC, and combined CE/T2W-MRC.

Segments	n	Sufficient visualization			p	
		T2W-MRC	CE-MRC	Combined CE/T2W-MRC	T2W-MRC vs. CE-MRC	Combined CE/T2W vs. T2W-MRC
CBD	56	50 (89.3%)	43 (76.8%)	55 (98.2%)	0.09	0.025
CHD	56	45 (80.4%)	46 (82.1%)	52 (92.9%)	0.782	0.014
RHD	53	35 (66.0%)	27 (50.9%)	44 (78.6%)	0.117	0.003
LHD	55	39 (70.9%)	25 (45.5%)	44 (78.6%)	0.004	0.025
Second branch of RHD	53	12 (22.6%)	7 (13.2%)	14 (25%)	0.096	0.157
Second branch of LHD	55	13 (23.6%)	7 (12.7%)	15 (26.8%)	0.058	0.157
Overall rating	56	37 (66.1%)	20 (35.7%)	40 (71.4%)	<0.001	0.025

Overall rating taking into account the total performance of CBD, CHD, RHD, and LHD.

CBD = common bile duct; CE-MRC = gadoteric acid-enhanced magnetic resonance cholangiography; CHD = common hepatic duct; LHD = left hepatic duct; RHD = right hepatic duct; T2W-MRC = T2-weighted magnetic resonance cholangiography.

Table 3  
Comparison of various liver function parameters and the overall rating of gadoxetic acid-enhanced MRC.

		Contrast-enhanced MRC		<i>p</i>
		Insufficient ( <i>N</i> = 36)	Sufficient ( <i>N</i> = 20)	
Child–Pugh score		7.17 ± 2.48	6.60 ± 2.06	0.541
MELD score		10.72 ± 4.79	9.95 ± 3.49	0.816
Total bilirubin (mg/dL)		1.54 ± 2.01	1.44 ± 1.34	0.431
Albumin (g/dL)		3.63 ± 0.63	3.52 ± 0.75	0.521
Child–Pugh Class	A or B	28 (77.8%)	16 (80.0%)	>0.99
	C	8 (22.2%)	4 (20.0%)	
Platelet count	Low	20 (55.6%)	15 (75.0%)	0.150
Prothrombin time	Prolonged	6 (16.7%)	4 (20.0%)	0.733
GOT	Abnormal	17 (47.2%)	12 (60.0%)	0.412
GPT	Abnormal	19 (52.8%)	11 (55.0%)	0.873

Child–Pugh score, MELD score, total bilirubin, and albumin value were expressed as mean ± standard deviation.

Low platelet count indicates a count of  $<150 \times 10^3/\mu\text{L}$ ; prolonged PT indicates a PT value of  $>12$  seconds; abnormal GOT or GPT indicates a level of  $>40$  U/L.

GOT = glutamic oxaloacetic transaminase; GPT = glutamic pyruvic transaminase; MELD = model for end-stage liver disease; MRC = magnetic resonance cholangiography; PT = prothrombin time.

#### 4. Discussion

The differences in the performance of T2W-MRC and CE-MRC may be due to the different imaging techniques. T2W-MRC benefits from a sufficiently long TE and displays only the fluid in the bile ducts with high signal intensity. When gadoxetic acid is used as a hepatobiliary contrast agent for functional imaging, it enhanced the biliary lumen via excretion into the bile ducts by a cellular process after its uptake by the hepatocyte.

Our results showed that the combination of T2W-MRC and CE-MRC provides better visualization of the biliary tree than T2W-MRC alone, especially for visualizing the CBD, CHD, and bilateral hepatic bile ducts. Gupta et al<sup>22</sup> reported that a combination of T2W images and gadolinium-enhanced T1W images during the hepatocyte phase is generally required for optimal evaluation of the biliary system in patients with normal liver function. CE-MRC can also increase the radiologist's confidence, especially in the evaluation of choledocholithiasis or identification of anatomic biliary ductal variants for living donors.<sup>13,16,17</sup>

We found that the combination of CE-MRC and T2W-MRC did not significantly improve visualization of small intrahepatic bile ducts of the bilateral second branches relative to T2W-MRC alone ( $p = 0.157$ ). In an attempt to improve visualization of the small intrahepatic bile ducts, Mangold et al<sup>16</sup> reported that second- and third-order bile ducts are more accurate in CE-MRC when delayed images are obtained 1.5 hours after the application of gadoxetic acid. In our study, the delay was only for 20 minutes, which might be the reason why the small intrahepatic bile ducts were poorly depicted in our study.

The overall rating of T2W-MRC was higher than that of CE-MRC alone in patients with liver cirrhosis for two reasons. It is well understood that decreased and delayed liver parenchymal enhancement is related to liver dysfunction, leading to

decreased excretion of gadoxetic acid into the biliary tract. In our study, only 35.7% of patients with liver cirrhosis had CE-MRC images with sufficient visualization of the biliary tree. Tschirch et al<sup>19</sup> also reported that in only about 40% of patients in the cirrhosis group the overall CE-MRC image quality was rated as sufficient for anatomical diagnosis within 30 minutes of contrast application. The second reason why the overall rating of CE-MRC was inferior to that of T2W-MRC is that enhancement of liver parenchyma decreases the contrast-noise ratio of the biliary tree. In an *in vivo* Phase I clinical evaluation performed in healthy volunteers receiving different doses of gadoxetic acid, Bollow et al<sup>23</sup> reported that low doses (10  $\mu\text{mol/kg}$ ) of gadoxetic acid were helpful for assessing the intrahepatic bile ducts. Further clinical studies are needed to determine whether low doses of gadoxetic acid improve the quality of CE-MRC images in patients with liver cirrhosis.

In our study, T2W-MRC images did not show the biliary tree in three patients. Studies have shown that signal loss in the bile ducts could be due to air bubbles, hemorrhage, or debris.<sup>24–26</sup> The possibility of signal loss due to air bubbles or hemorrhage in our study was excluded on abdominal ultrasound and conventional T1W, T2W, and dynamic MRI. Thick bile inside the biliary tree is the most likely reason for lack of visualization. Interestingly, there was sufficient visualization on CE-MRC images in two of the three patients. We suggest that the hepatobiliary phase of T1W MRI with gadoxetic acid might be a complementary method in clinical practice, especially when T2W-MRC images are inconclusive.

In this study, we evaluated the relationship between various laboratory data representing liver function and the overall rating of CE-MRC. We found that although the number of images with insufficient visualization tended to be higher in patients with Child–Pugh classification C, higher Child–Pugh scores, higher MELD scores, and higher total bilirubin levels, there were no significant differences between liver function parameters and visualization quality. One reason for this may be that there were few patients with Child–Pugh classification C in our study. In addition, few studies have evaluated the relation between various laboratory parameters of liver function and the uptake and excretion of gadoxetic acid in patients with liver cirrhosis.<sup>19,27–29</sup> Their results showed disagreements about the relationships between laboratory parameters and the uptake or excretion of gadoxetic acid. Even Motosugi et al<sup>27</sup> reported that no biological markers of liver function are significantly correlated with liver enhancement.

We acknowledge that our study had the following limitations. First, hepatocyte phase imaging was performed 20 minutes after the injection of contrast agent. A longer delay may be needed for patients with liver cirrhosis. The optimal timing for biliary imaging in patients with impaired liver function should be studied in the future. Second, liver cirrhosis was not histologically confirmed in all the patients.

In conclusion, CE-MRC is not superior to conventional T2W-MRC in biliary visualization in patients with liver cirrhosis. However, a combination of T2W-MRC and CE-MRC provides significantly better visualization of biliary structures than T2W-MRC alone. The hepatobiliary phase of

T1W MRI with gadoteric acid might be a complementary method in clinical practice, especially when T2W-MRC images are inconclusive.

### Acknowledgments

The authors would like to thank the National Science Council, Taiwan, R.O.C., for financially supporting this research (Contract No. NSC100-2314-B-010-012-MY2).

### References

- Wallner BK, Schumacher KA, Weidenmaier W, Friedrich JM. Dilated biliary tract: Evaluation with MR cholangiography with a T2-weighted contrast-enhanced fast sequence. *Radiology* 1991;**181**:805–8.
- Dwerryhouse SJ, Brown E, Vipond MN. Prospective evaluation of magnetic resonance cholangiography to detect common bile duct stones before laparoscopic cholecystectomy. *Br J Surg* 1998;**85**:1364–6.
- Miletic D, Uravic M, Mazur-Brbac M, Stimac D, Petranovic D, Sestan B. Role of magnetic resonance cholangiography in the diagnosis of bile duct lithiasis. *World J Surg* 2006;**30**:1705–12.
- Guibaud L, Bret PM, Reinhold C, Atri M, Barkun AN. Bile duct obstruction and choledocholithiasis: diagnosis with MR cholangiography. *Radiology* 1995;**197**:109–15.
- Barish MA, Soto JA. MR cholangiopancreatography: techniques and clinical applications. *AJR Am J Roentgenol* 1997;**169**:1295–303.
- Fulcher AS, Turner MA. Pitfalls of MR cholangiopancreatography (MRCP). *J Comput Assist Tomogr* 1998;**22**:845–50.
- Irie H, Honda H, Kuroiwa T, Yoshimitsu K, Aibe H, Shinozaki K, et al. Pitfalls in MR cholangiopancreatographic interpretation. *Radiographics* 2001;**21**:23–37.
- David V, Reinhold C, Hochman M, Chuttani R, McKee J, Waxman I, et al. Pitfalls in the interpretation of MR cholangiopancreatography. *AJR Am J Roentgenol* 1998;**170**:1055–9.
- Papanikolaou N, Prassopoulos P, Eracleous E, Maris T, Gogas C, Gourtsoyannis N. Contrast-enhanced magnetic resonance cholangiography versus heavily T2-weighted magnetic resonance cholangiography. *Invest Radiol* 2001;**36**:682–6.
- Fayad LM, Holland GA, Bergin D, Iqbal N, Parker L, Curcillo 2nd PG, et al. Functional magnetic resonance cholangiography (fMRC) of the gallbladder and biliary tree with contrast-enhanced magnetic resonance cholangiography. *J Magn Reson Imaging* 2003;**18**:449–60.
- Fayad LM, Kamel IR, Mitchell DG, Bluemke DA. Functional MR cholangiography: diagnosis of functional abnormalities of the gallbladder and biliary tree. *AJR Am J Roentgenol* 2005;**184**:1563–71.
- Ergen FB, Akata D, Sarikaya B, Kerimoglu U, Hayran M, Akhan O, et al. Visualization of the biliary tract using gadobenate dimeglumine: preliminary findings. *J Comput Assist Tomogr* 2008;**32**:54–60.
- Carlos RC, Hussain HK, Song JH, Francis IR. Gadolinium-ethoxybenzyl-diethylenetriamine pentaacetic acid as an intrabiliary contrast agent: preliminary assessment. *AJR Am J Roentgenol* 2002;**179**:87–92.
- Dahlstrom N, Persson A, Albiin N, Smedby O, Brismar TB. Contrast-enhanced magnetic resonance cholangiography with Gd-BOPTA and Gd-EOB-DTPA in healthy subjects. *Acta Radiol* 2007;**48**:362–8.
- Lee MS, Lee JY, Kim SH, Park HS, Kim SH, Lee JM, et al. Gadoteric acid disodium-enhanced magnetic resonance imaging for biliary and vascular evaluations in preoperative living liver donors: comparison with gadobenate dimeglumine-enhanced MRI. *J Magn Reson Imaging* 2011;**33**:149–59.
- Mangold S, Bretschneider C, Fenchel M, Seeger A, Kramer U, Klumpp B, et al. MRI for evaluation of potential living liver donors: a new approach including contrast-enhanced magnetic resonance cholangiography. *Abdom Imaging* 2012;**37**:244–51.
- Reiner CS, Merkle EM, Bashir MR, Walle NL, Nazeer HK, Gupta RT. MRI assessment of biliary ductal obstruction: is there added value of T1-weighted gadolinium-ethoxybenzyl-diethylenetriamine pentaacetic acid-enhanced MR cholangiography? *AJR Am J Roentgenol* 2013;**201**:W49–56.
- Cieszanowski A, Stadnik A, Lezak A, Maj E, Zieniewicz K, Rowinska-Berman K, et al. Detection of active bile leak with Gd-EOB-DTPA enhanced MR cholangiography: comparison of 20–25 min delayed and 60–180 min delayed images. *Eur J Radiol* 2013;**82**:2176–82.
- Tschirch FT, Struwe A, Petrowsky H, Kakales I, Marincek B, Weishaupt D. Contrast-enhanced MR cholangiography with Gd-EOB-DTPA in patients with liver cirrhosis: visualization of the biliary ducts in comparison with patients with normal liver parenchyma. *Eur Radiol* 2008;**18**:1577–86.
- Oberti F, Valsesia E, Pilette C, Rousselet MC, Bedossa P, Aube C, et al. Noninvasive diagnosis of hepatic fibrosis or cirrhosis. *Gastroenterology* 1997;**113**:1609–16.
- Kamath PS, Kim WR, Advanced Liver Disease Study Group. The model for end-stage liver disease (MELD). *Hepatology* 2007;**45**:797–805.
- Gupta RT, Brady CM, Lotz J, Boll DT, Merkle EM. Dynamic MR imaging of the biliary system using hepatocyte-specific contrast agents. *AJR Am J Roentgenol* 2010;**195**:405–13.
- Bollow M, Taupitz M, Hamm B, Staks T, Wolf KJ, Weinmann HJ. Gadolinium-ethoxybenzyl-DTPA as a hepatobiliary contrast agent for use in MR cholangiography: results of an *in vivo* Phase-I clinical evaluation. *Eur Radiol* 1997;**7**:126–32.
- Watanabe Y, Dohke M, Ishimori T, Amoh Y, Okumura A, Oda K, et al. Diagnostic pitfalls of MR cholangiopancreatography in the evaluation of the biliary tract and gallbladder. *Radiographics* 1999;**19**:415–29.
- Pavone P, Laghi A, Panebianco V, Catalano C, Passariello R. MR cholangiopancreatography: technique, indications and clinical results. *Radiol Med* 1997;**94**:632–41.
- Pavone P, Laghi A, Panebianco V, Catalano C, Lobina L, Passariello R. MR cholangiography: techniques and clinical applications. *Eur Radiol* 1998;**8**:901–10.
- Motosugi U, Ichikawa T, Sou H, Sano K, Tominaga L, Kitamura T, et al. Liver parenchymal enhancement of hepatocyte-phase images in Gd-EOB-DTPA-enhanced MR imaging: which biological markers of the liver function affect the enhancement? *J Magn Reson Imaging* 2009;**30**:1042–6.
- Tamada T, Ito K, Higaki A, Yoshida K, Kanki A, Sato T, et al. Gd-EOB-DTPA-enhanced MR imaging: evaluation of hepatic enhancement effects in normal and cirrhotic livers. *Eur J Radiol* 2011;**80**:e311–6.
- Tamada T, Ito K, Sone T, Kanki A, Sato T, Higashi H. Gd-EOB-DTPA enhanced MR imaging: evaluation of biliary and renal excretion in normal and cirrhotic livers. *Eur J Radiol* 2011;**80**:e207–11.